

Active Systems: Phase Transitions and Work



Department of Physics, University of Warwick, Coventry CV4 7AL, United Kingdom

Immersing an asymmetric rotor in an active system sets it into spontaneous rotation. This report aims to investigate the factors affecting rotation in an active bath. Firstly, we focus on phase transitions in the Vicsek model in order to understand the physics of active systems. Throughout the results, a potentially novel phase transition is observed for the topological Vicsek model. Secondly, the rotors are placed in different active baths and their rotations are investigated. An empirical relationship is found between order in the system and rotation, emphasising that collective motion enhances rotation. Finally, the shapes of the rotors are optimised using a genetic algorithm for the different baths.

I. Introduction

Active systems contain particles that move 'actively' by absorbing energy from their environment, driving the system far away from equilibrium [1]. Examples include swarms of fish [2], animal herds [3], bacterial colonies [4] and other microorganisms [5]. These are often used as models to explain and understand non-equilibrium physics. An important example of an active system is one which consists of self-propelled agents, where the absorbed energy is converted into directed motion [6]. These systems were traditionally studied to explore swarm behaviour occurring in

nature, with Craig Reynolds introducing his 'Boids' computer programme to simulate birds, animals and fish [7]. Vicsek *et al.* [8] followed with the most seminal work on self-propelled particles, by introducing the Vicsek model. Research in the field has largely excelled since then, particularly in creating self-propelling artificial agents in order to use their properties for doing useful work. For example in [9] it was shown that rod-shaped particles can swim in an aqueous hydrogen peroxide solution by catalysis of oxygen at the Pt rod-end. This demonstrated the possibility of self-propulsion by local energy conversion. Ar-

tificial swimmers can also be powered by external fields, as shown in [10], where the application of a magnetic field leads semiflexible rods to resemble the motion of biological self-propelled agents such as spermatozoa.

The applications of active systems emerge in many modern problems such as, biomedicine [11] [12] or environmental sustainability [13]. An important problem is harnessing the energy that is absorbed by the agents in a useful manner. Research has been conducted to investigate the rectification of work done by active matter by: immersing microscopic gears in bacterial active systems [14] [15] or by creating a wall of funnels to concentrate the population of bacteria [16]. Taking inspiration from the research done on this topic, a question was asked: What factors affect the energy that is harnessed?

II. Theory

With the overall purpose of investigating the factors that affect harnessed energy, there is a need to understand the physics of active systems in the first place. Therefore, an introduction to the differences between interacting and non-interacting particles is presented.

A. Non-interacting Particles

As previously explained, the motion of self-propelled particles arises from their ability to absorb energy from the environment. Compared to passive Brownian particles, whose motion is due to the random collisions with the surrounding molecules [17], self-propelled particles have a self-propulsion term, hence making them active Brownian particles. Their motions look similar to each other but the active particles' motion is irreversible.

Active Brownian particles can be governed by rotational diffusion dynamics; where the particle's velocity modulus is constant and its orientation undergoes free diffusion. Janus particles can exhibit this motion as they have two sides with different physical and/or chemical properties; with each side being able to interact differently with the environment. For instance, in [18] and [19] the motion of the Janus particles is produced by absorption of the laser from the metal side of agents.

Active particles can also be governed by run-and-tumble dynamics. These were introduced to explain the motion of *E. coli* bacteria [20] [21]. A run-and-tumble particle has a random path which consists of alterations between straight runs and Poisson distributed reorientations [22].

Both of these models are valid for only spherically or axially symmetric active par-

ticles. However, most agents considered in research, including in this report, have spherical or axial symmetry [23]. For more information on the dynamics of non-spherical Brownian active particles, see section II.B.3 of [23].

Even though the dynamics of non-interacting active particles are well understood, natural and artificial active agents are more often found in environments where they are not isolated. Interactions change the particle's dynamics and can give rise to cooperative behaviour [23]. Aligning interactions are particularly important as they can cause collective motion.

B. Collective Motion

Collective behaviour needs to satisfy two conditions: (i) an individual's actions are dominated by its neighbours and (ii) all the individuals in the collective simultaneously change their behaviour to a common pattern [24]. Collective motion is a manifestation of collective behaviour where the common pattern is motion.

Most mathematical models proposed for collective motion study are consequent variations of the boids computer program by Craig Reynolds [7]. This model builds on the three simple rules, shown in Fig. 1, that

- agents must avoid collision with neighbours

- agents must attempt to match direction of velocity with neighbours
- agents must attempt to stay close to neighbours

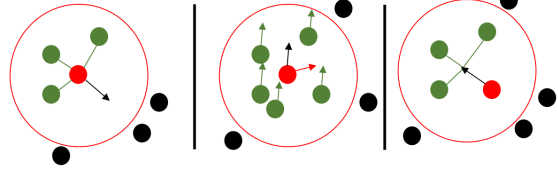


Figure 1: The basic rules of collective motion in Reynolds' boids computer program [7]. *Separation* (left) - the red agent aims to avoid collision with green neighbours within range of interaction. *Alignment* (center) - the red agent tries to match the average direction of green neighbours in range of interaction. *Cohesion* (right) - the red agent tries to stay close to green neighbours within range of interaction. Adapted from [25].

1 The Vicsek Model

The seminal work on collective motion of self-propelled particles was done by Tamás Vicsek's in 1995 [8]. Here, N identical self-propelled agents have a constant magnitude in velocity, and at each time step, each agent assumes the average direction of motion of itself and its neighbouring agents, within a radius, R . There is random noise added to the orientation of the aligned velocity between $-\eta/2$ and $\eta/2$. The position of each particle i , where i is $i = 1, 2, \dots, N$, at each new time step ($t + 1$), is determined by

$$\mathbf{r}_i(t + 1) = \mathbf{r}_i(t) + \mathbf{v}_i(t)\Delta t \quad (1)$$

In two spatial dimensions ($d = 2$), $\mathbf{v}_i(t)$ is such that, the magnitude in velocity, v , is kept constant whilst the direction, θ_i , is changed according to

$$\theta_i(t+1) = \langle \theta(t) \rangle_R + \Delta\theta \quad (2)$$

Here, $\langle \theta(t) \rangle_R$ is the average direction of motion of all particles, including particle i , within a radius R . $\Delta\theta$ is the random noise that represents an external perturbation. It takes into account usual stochastic and deterministic factors [26] affecting collective motion, as this is a model initially intended for the study of flocks. Using these equations of motion, the agents in the Vicsek model obey rotational diffusive dynamics with an alignment interaction.

The Vicsek model has a metric method of choosing which neighbours to interact with. Therefore, each agent interacts with neighbours that are within R . For example, as shown in Fig. 2, when $\eta = 0$, the red agent has averaged its direction depending on the neighbours within R .

The existence of perturbations in the Vicsek model suggests that they may hinder the process of self-organisation of the system. Therefore, a barrier should exist between the two phases: (i) the flock being in disordered state (velocities of agents are random) and (ii) the flock being in an ordered state (velocities of agents are in the same direction). This movement from one

state to another can be associated with a phase transition.

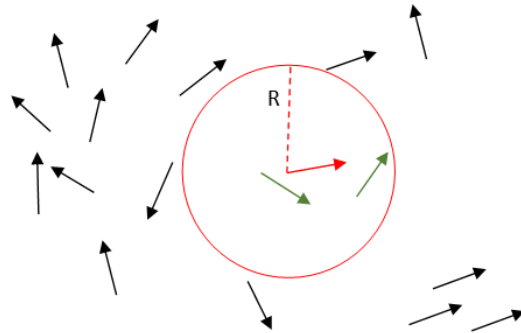


Figure 2: An example of a particle aligning its orientation with its neighbours in the Vicsek Model. An agent (red), takes the average direction of the agents within its radius R (green). It does not interact with the agents outside the radius (black).

2 Phase Transitions

Phase transitions are important because they can give physicists a range of information about a system. A common phase transition is the transformation of water e.g. the freezing of water, when the control parameter, temperature, is decreased. The phase transition is defined by observation of the order parameter [27], which changes continuously or discontinuously as the control parameter is varied. The variation of the order parameter defines a symmetry breaking in the system.

Phase transitions can be first order, where there is a discontinuity in the order parameter at the critical state [27]. For the example with water, there is a discontinu-

ity in the density property of the system as it freezes or evaporates. Phase transitions can also be second order, where the order parameter changes continuously. An example is the ferromagnetic phase transition of iron where, as temperature is increased, the magnetisation decreases continuously [27].

The average velocity is the most appropriate order parameter used for collective motion and is defined by

$$\psi = \frac{1}{Nv} \left| \sum_{i=1}^N \mathbf{v}_i \right| \quad (3)$$

Where v is the magnitude of constant velocity of agents in the model, N is the number of agents, and \mathbf{v}_i is the velocity of each agent i [27]. Initially as the system is in a disordered phase, all of the orientations will have a random direction, with an error of $1/\sqrt{N}$, and hence $\psi \rightarrow 0$. As the system transitions to an ordered phase, the agents synchronise their directions, so $\psi \rightarrow 1$.

Vicsek *et al.* showed two phase transitions by varying noise and density as control parameters. They suggested that there is an apparent second order phase transition as shown in Fig. 3a. In the presence of no noise, the collective achieves ordered motion with $\psi = 1$, but as the perturbations are increased, the ordered motion decreases. When the density is varied, a phase transition is again observed as in Fig. 3b. At low density, the agents are not able to synchronise their directions, as they are

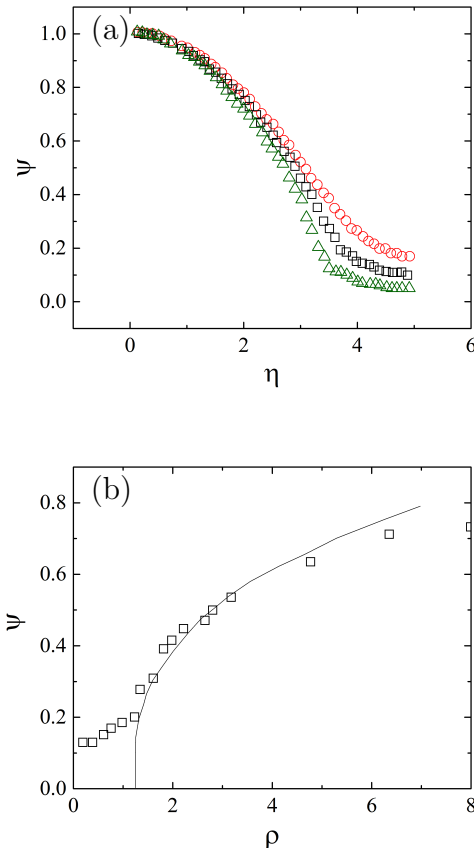


Figure 3: Effect of varying noise (a) and density (b) as control parameters on the order parameter ψ , resulting in phase transitions. (a) Each symbol corresponds to \circ : $L = 3.1, N = 40$; \square : $L = 5, N = 100$; \triangle : $L = 10, N = 400$. The density is kept constant at $\rho = 4 L^{-2}$. (b) The phase transition, when varying density as a control parameter, $\eta = 2$. Both adapted from [8].

not within a radius of interaction, but as the density increases the agents are able to align.

There has been vigorous debate over whether the phase transition in the Vicsek Model is indeed second order. Firstly questioned by Chaté and Grégoire [28], it was argued that in 2-d, the phase transition is always first order. Following this, Nagy *et al.* argued that the transition is second order for $v < 0.1$, but for larger velocities,

the transition is first order [29]. Chaté and Ginelli disagreed and argued that the velocity is also first order for small velocities [30]. Evidently, there was disagreement about the nature of the phase transition but now it is widely accepted to be first order [31].

3 Alterations of the Vicsek Model

Sensory or cognitive abilities of real agents need to be considered for an improved model of a biological swarm. Therefore, an alteration that is worth considering is changing the interactions neighbourhood. For example, the Vicsek metric model is challenged in one of the largest experiments engineered for the purpose of analysing birds, where Ballerini *et al.* showed that bird flocks interact topologically [32] with 6/7 closest agents as shown in Fig. 4. In comparison to the metric model, Fig. 2, where the particle communicates with all agents within a set radius R , in the topological model, each particle communicates only with its k closest neighbours.

An intriguing difference between the two models is that the topological model obtains a second order phase transition, when varying the noise as a control parameter [33]. This is due to phase separation being removed in topological models causing the transition to be continuous. In comparison, in metric models the phase separation still exists, giving rise to a discontinuity,

which becomes more obvious at larger system sizes.

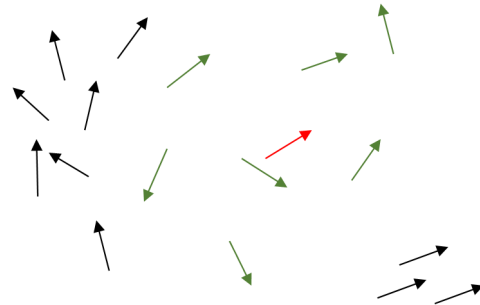


Figure 4: An example of a particle aligning its orientation with its neighbours in the topological model. A red agent takes the average direction of the green 7 closest neighbours.

Another possible alteration is adding the noise in different ways. At finite sizes, the phase transition varies when investigated with two different perturbations: intrinsic noise and extrinsic noise. The intrinsic noise is the original variation used in the Vicsek Model - adding the perturbation once the average direction has been calculated. The idea of extrinsic noise, also known as vectorial [28], is when the direction of movement of each particle is perturbed before averaging. As explained in [30], the extrinsic noise phase transition is much steeper than the original Vicsek intrinsic noise phase transition.

The fact that particles do not have any repulsive force between each other can cause them to overlap, which can be considered a limitation. A suitable alteration would be to add a repulsive force which would prevent this. As addressed

in [34], a force can be imposed on the agents that ensures that an equilibrium distance is kept through attractive and repulsive forces. This is also done to ensure cohesion, a problem of both topological and metric models. Another example of introducing repulsion is in [35], where a short-range repulsive force is incorporated without aligning interactions. Furthermore, in [30] a short range repulsive force is introduced simply to impede the agents from overlapping and will be used in this report.

C. Mixture of Active and Passive particles

After investigating simple systems of active particles, gears will be immersed in the system and they will be considered to act as passive objects. This requires an understanding of the interactions between active and passive particles in a system.

A passive particle is said to be immersed in an active bath when there is a significant amount of active agents. These will exert non-thermal forces on the passive particle, changing its dynamics [23]. For instance, a passive colloidal particle in a bacterial active bath behaves as an active particle due to the many interactions with its neighbours [36]. Another example is that the passive particles can start interacting with each other due to the active agents, as can be seen in [37].

D. Rotors

Passive particles that do not have a spatial symmetry can experience directed motion when in an active bath. For example when a wedge is surrounded by passive particles, it remains stationary because equal pressure is exerted on all sides, Fig. 5a. In an active bath, particles will exert sufficient force on the wedge when colliding, so that there is a force equal and opposite to the black arrow in Fig. 5c, causing the particle to align its velocity with the wall. This will cause particles to effectively accumulate inside the wedge, as in Fig. 5b, driving it into motion.

It was first noticed by Curie [14] that an asymmetric effect causes rectification. In this case, unidirectional motion is the rectification, where time and spatial inversion are broken. The time asymmetry is caused by the self-propulsion of the agents that are out-of-equilibrium and are therefore time-irreversible. The wedge placed in the active bath provides the spatial asymmetry.

This unidirectional motion has already been explored in [38], where it was shown that a passive wedge undergoes motion in an active bath. The motion was maximised at an intermediate density, which was explained by the fact that at low density, there are too few agents hitting the wedge, and at high density, the wedge becomes jammed and cannot move efficiently. Here

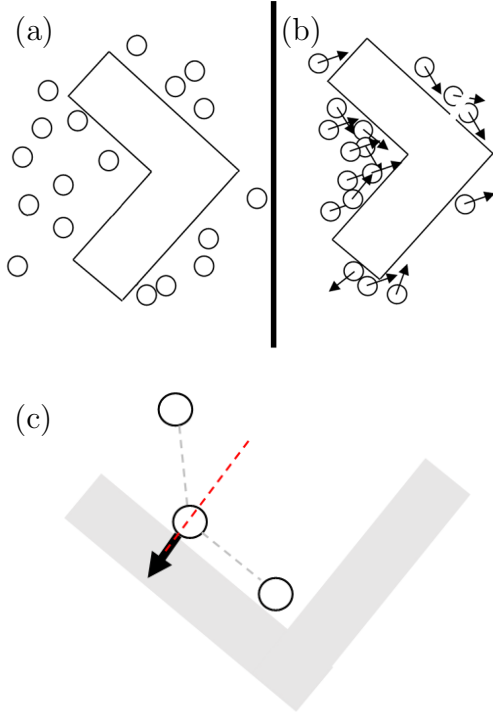


Figure 5: Schematic diagram of a wedge interacting with particles. (a) The particles are passive and exert equal pressure on all sides causing the wedge to be stationary. (b) Active particles accumulate in the cusp due to their self-propulsion and move the wedge. The arrows represent their self-propulsive nature. Adapted from [23]. (c) An active particle colliding with the cusp of a wedge. As the particle comes in with enough force, there is a force from the wall equal and opposite to the black arrow, towards the normal (red line) which aligns the velocity of the particle parallel to the wall. Adapted from [14].

the angle of the wedge was maximised to 90 degrees in order to achieve maximum mobility. In contrast to this paper, in [39], a round wedge was found to also have pronounced directed motion even at low densities. Finally, in [40], the optimal shape of a wedge was found to be U-shaped rather than V-shaped.

Considering that the optimization of the mobility of wedges in an active bath has

been investigated in detail, what is of bigger interest are ratchet wheels, which exhibit random rotation when in an active bath. The idea for these shapes and the fact that a ratchet wheel placed in a thermal bath will not exhibit rotation is considered in Feynman's Ratchet and Pawl thought experiment [41]. This is because the particles are passive and time symmetry is not broken. Similarly to the wedge example in Fig. 5, passive particles will not clump inside the teeth of the rotor in Fig. 6a, so it will not rotate. Contrastingly, active particles will clump in the teeth of the rotor as shown in Fig. 6b, because time inversion and spatial symmetry are both broken due to the self-propulsion of the particles and the asymmetric shape of the rotor, respectively. Both of those conditions need to be satisfied for unidirectional rotation to occur; therefore, a symmetric rotor should not exhibit rotation.

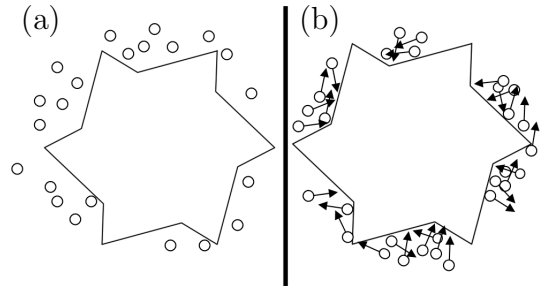


Figure 6: Schematic diagram of a rotor in (a) a passive bath of particles and (b) an active bath of particles. (a) The particles exert equal pressure on all sides so rotor is stationary. (b) Active particles accumulate in the teeth due to their self-propulsion and spin the rotor.

In [42], Angelani *et al.* show through a simulation that an asymmetric object can be set into spontaneous rotation by being immersed in a chaotic bacterial bath. Following this, Di Leonardo *et al.* [14], prove the results experimentally with a bacterial bath.

Sokolov *et al.* [15] provide experimental results for the rectification of these non-equilibrium active real systems and also mention that this can be enhanced by making use of the collective motion of bacteria. Other studies of this are described in [43], where the rotation of several different gears due to self-propelled robots is investigated or in [44] where the same experiment is performed with Janus colloids.

Taking inspiration from the research done so far, the potential for rectification of a system made up of a rotor and active matter will be investigated in this report. However, first a simpler active system will be composed without any rotors in it. This allows for thorough investigation of the physics governing active systems, in particular related to phase transitions. Following on, systems with Vicsek and topological alignment interactions will be compared in order to find consistencies between the models. A rotor will be immersed in several active baths to investigate which factors affect the amount of energy that can be harnessed in these systems. The Vicsek phase transition will be

compared to a novel phase transition, with rotation as an order parameter. In light of the previously mentioned investigations, where an optimal angle [38] and optimal shape [40] for a moving wedge was found, an obvious factor of rotation is the shape of the rotor. This will be optimised for each active bath using a genetic algorithm, allowing us to compare the optimal shapes between different baths.

III. Methodology

A. Code Details

The whole project simulation was written in Python, due to its simplistic data-structures and its object-oriented nature. Furthermore, it has multiple useful libraries, which were helpful in mathematical manipulation and execution of the code, such as Shapely, Numpy, Matplotlib and Pandas. The systems for computations were a server based on 24 Intel® Xeon® X5650 Processors and personal computers. For the complete code simulation see [45].

B. Active Systems

Boundary conditions were used for all models as this ensured that cohesion is maintained. A box of size L was populated with N particles with random orientations of velocities and random positions. The velocity of the agents was $v = 0.05$, the radius of in-

teraction $R = 1$, $\rho = \frac{N}{L^2}$ always and time increment from Eq. 1, $\Delta t = 1$. Simulations were ran for U time units depending on which results were being taken.

Ensemble averages were taken throughout the whole simulation even though time averages were also considered. The system is ergodic but this is only observed at long time steps, U . This is because the particles need a significant amount of time to explore all phase-space. Observing Fig. 7, at few time steps, when the system is not given enough time to stabilise, the time averages do not match the ensemble averages. However, if the time averages are taken after many time steps, the data points for time and ensemble averages coincide.

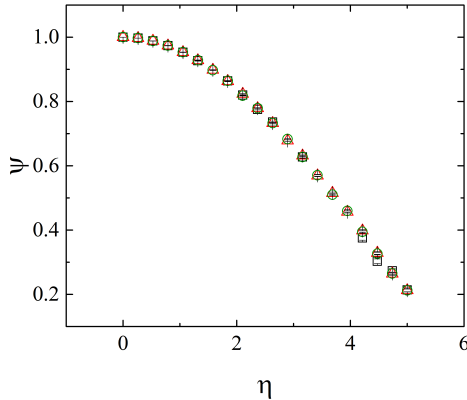


Figure 7: Ergodicity for the Vicsek Model. At few time steps, $U = 500$ (\square) the data does not match the ensemble averages (\triangle) but at many time steps, $U = 20,000$ (\circ) the ensemble averages are matched. Parameters are $\rho = 4$, $L = 3.1$, $N = 40$. Both time averages were taken across 500 repeats, and ensemble averages were taken across 461 repeats.

C. Rotors

The rotors were built using the following parameters: spikes (S), inner radius (a), outer radius (b), angle shift (ϵ). As seen on Fig. 8a, S points are positioned equidistantly on the surface of a circle of radius b from the centre of the box. Then S points are added at a distance a from the centre of the box as shown in 8b. The inner points are then shifted by an angle ϵ as seen in 8c. The positions of all points are sorted in an array depending on what angle they form with the horizontal. They are finally linked consequentially as seen in 8d.

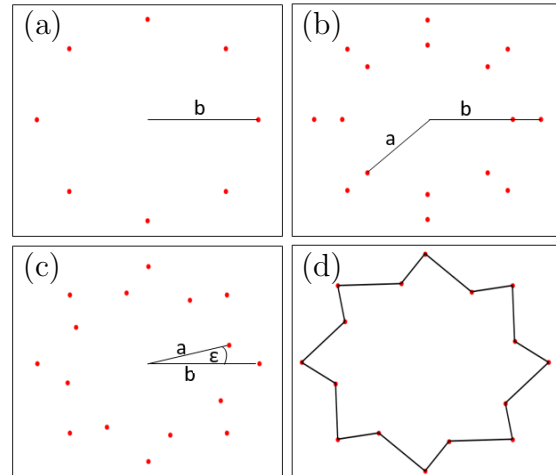


Figure 8: The process of building a rotor. (a) S points are positioned equidistantly on the surface of a circle of radius b . (b) S points are positioned equidistantly on the surface of a circle of radius a . (c) Inner points are shifted by an angle ϵ . (d) The points are linked consequentially to form a rotor.

The rotors were held fixed at the centre of the box at $L/2, L/2$ and allowed to rotate depending on the forces experienced by all the agents. It is appropriate to now

introduce the equations governing the motion of the particles. First, the position of each particle is updated as in the Vicsek model by Eq. 1. The velocity is rewritten to be updated as

$$\mathbf{v}_i(t+1) = \mathbf{v}_i(t) + \frac{\mathbf{F}_{\text{tot}}^i}{m} \Delta t \quad (4)$$

This allows for the different forces to be implemented with ease. Here, m is the mass of each particle kept at 1, $\mathbf{v}_i(t+1)$ is the velocity at $(t+1)$, $\Delta t = 1$ and $\mathbf{F}_{\text{tot}}^i$ is the total force on particle i defined by

$$\begin{aligned} \mathbf{F}_{\text{tot}}^i = & \alpha \mathbf{F}_{\text{alignment}}^i + \beta \sum_{j=1, i \neq j}^N \mathbf{F}_{\text{repulsive}}^{ij} \\ & + \gamma \mathbf{F}_{\text{object}}^i + \mathbf{F}_{\text{noise}}^i \end{aligned} \quad (5a)$$

The total force on each particle constitutes of several other forces. $\mathbf{F}_{\text{noise}}^i$ is the error force on particle i as applied in the Vicsek model. $\mathbf{F}_{\text{alignment}}^i$ is the force on a particle which makes it align with its neighbours, either with Vicsek or topological interactions. $\mathbf{F}_{\text{repulsive}}^{ij}$ is the repulsive force on i due to j , which is defined below as previously mentioned in the introduction [30]

$$\mathbf{F}_{\text{repulsive}}^{ij} = \frac{\mathbf{e}_{ij}}{1 + e^{\frac{|\mathbf{r}_j - \mathbf{r}_i|}{r_c}}} \quad (6)$$

Where r_c is the repulsive range set to $v\Delta t$. $|\mathbf{r}_j - \mathbf{r}_i|$ is the distance between i and j and \mathbf{e}_{ij} is the unit vector from i to j .

Next, the $\mathbf{F}_{\text{object}}^i$ is the force by the ob-

ject on particle i , defined by

$$\mathbf{F}_{\text{obj}}^i = (\hat{n} \bullet \mathbf{v}_i) \hat{n} \quad (7)$$

Where, \hat{n} is the normal vector from the surface of the object and \mathbf{v}_i is the velocity vector. This is the force as defined for active particles interacting with the wedge in the introduction, from [14].

All forces, but $\mathbf{F}_{\text{noise}}^i$, are preceded by some constant which determined their strength. Furthermore, forces can efficiently be turned-off in this way. In particular, when investigating systems with and without alignment, the parameter α can be set to 0 for no alignment interactions and set to 1 for alignment interactions between the particles.

The moment of inertia $I = 167$ is chosen in consideration of the mobility of the rotor. If it is too small, the rotor turns vigorously and if it is too large, the rotor does not exhibit movement. A resistive force is also added equivalent to $\mathbf{F}_{\text{resistive}} = 0.2\omega$. The active bath for the rotors was $N = 25$, $L = 5$, both chosen for computational simplicity since all densities induce some rotation, as mentioned in introduction.

D. The Genetic Algorithm

The genetic algorithm is used for the optimisation of the shape of the rotor. The principle is inspired from natural selection. The algorithm creates an initial population,

and then a sequence of new populations at each 'generation' where the new population is created from the old by:

1. Calculating the raw score of each population member.
2. Scaling each raw score to an expectation value.
3. Selecting two parents and producing a child based on expectation values. For each parameter of the child a parameter from one of the two parents is chosen at random.
4. Repeating previous step according to the number of members in the initial population.
5. Mutating one of the child's parameters randomly based on a mutation rate.

Any parameter of the child has a 1% chance of mutation to a different value taken from a range of parameters to ensure variety. A population of 30 is initialised, again to ensure variation. The score, which was chosen as a basis for picking 'fittest' members of the population, was positive angular displacement averaged over 96 runs (due to the system model, 24 core, and ability to parallelise the runs). The members of the population were created randomly using the parameters for building rotors mentioned in Section III.C. Minimum and maximum values of all parameters were cho-

sen in order to prevent the genetic algorithm for picking unreasonable random values. The mutation parameters were also chosen from the same parameter ranges. Below is a table, for all parameters with their ranges. It is acknowledged that some subjectivity is included for choosing the parameter ranges. The outer radius is kept constant as we are investigating shapes of rotors rather than size.

Parameter	Range (unit length)
Inner Radius (a)	$a \in \mathbb{R} 0.1 \leq a < 0.2L$
Outer Radius (b)	$0.2L$
Angle Shift (ϵ)	$\epsilon \in \mathbb{R} 0 \leq \epsilon < 2\pi$
Spikes (S)	$S \in \mathbb{Z} 5 \leq S \leq 15$

Table 1: All parameter ranges for creating each population member in genetic algorithm and choosing mutation values

IV. Results

A. Active Systems

The simple case of no gears in the system is first considered. The Vicsek model is used for the interactions between the particles. A phase transition is observed in Fig. 9a as the noise is varied. At low noise, the agents are in ordered motion, as expected, and at high noise the active agents fail to synchronise their directions.

These results encouragingly agree with the data in Fig. 3a. A small difference between 9a and 3a can be noticed, in particular that the values in Fig. 3a are steeper. It has been acknowledged that there have

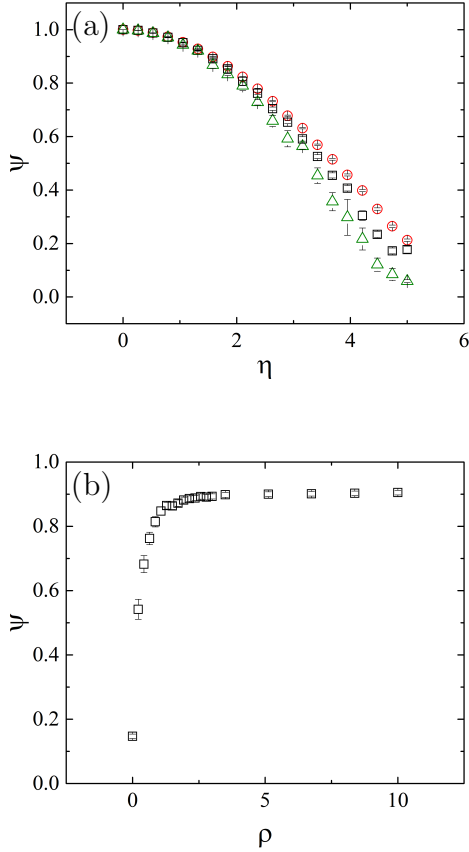


Figure 9: Phase transitions in the Vicsek model. (a) Effect of noise as a control parameter on the order parameter ψ . Each symbol corresponds to \circ : $L = 3.1$, $N = 40$, 461 ensemble averages; \square : $L = 5$, $N = 100$, 41 ensemble averages; \triangle : $L = 10$, $N = 400$, 3 ensemble averages. The density is kept constant at $\rho = 4L^{-2}$. (b) The phase transition for a system at $\eta = 2$ when varying density as a control parameter. Here 101 ensemble averages were taken. ρ is in units of L^{-2} .

been problems with the results from [8], therefore the close resemblance is satisfactory. Due to computational limitations, higher system sizes were unable to be simulated as computation time scales as N^2 .

Surprisingly, this self-propelled particle system is extremely similar to the Ising model of ferromagnetic phase transition [27] which is first order. In it, the magneti-

sation (order parameter) decreases continuously, as the temperature (the control parameter) is increased above the Curie temperature (the critical point). In particular, here it can be observed that as the system sizes increase from $N = 40 \rightarrow N = 400$, the phase transition becomes steeper which points towards a potential resemblance to a Curie phase transition with larger system sizes.

Following the findings of Ballerini *et al.* [32], as mentioned in the introduction, it was observed that the interactions between flocks were topological rather than metric. Changing the interaction between the agents to topological, with seven nearest neighbours in accordance with [32], resulted in Fig. 10a. The variation of the noise control parameter induces a phase transition. As mentioned in the theory, due to the absence of phase separation, the transition for this model is expected to be second order. The transition appears steeper; however, without simulations of larger systems this cannot be confirmed. As density is varied in Fig. 10b, no phase transition can be observed as expected. This is because the model is metric-free and varying the density should not cause an effect on how the agents align; in other words an agent always looks at the closest seven neighbours, no matter how dense the active bath is.

Given this observation, it was asked

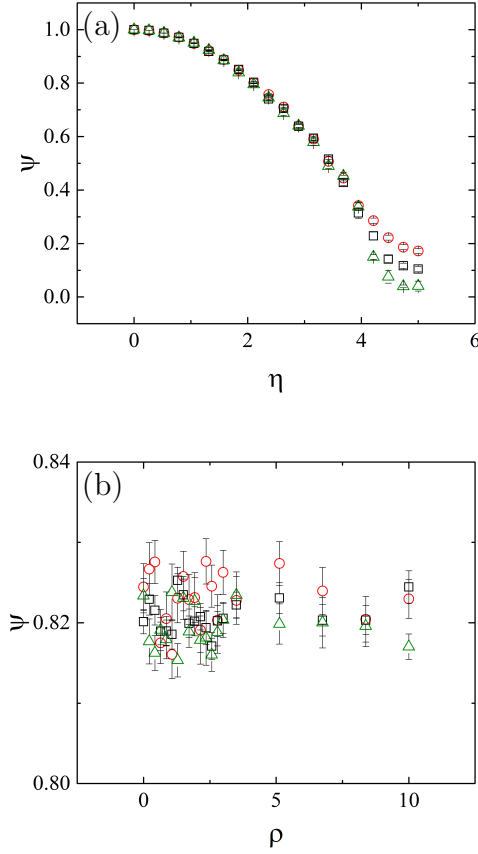


Figure 10: Phase transitions in the topological model. (a) Effect of varying noise as a control parameter on order parameter ψ . Each symbol corresponds to \circ : $L = 3.1, N = 40$, 101 ensemble averages; \square : $L = 5, N = 100$, 31 ensemble averages; \triangle : $L = 10, N = 400$, 4 ensemble averages. The density is kept constant at $\rho = 4 L^{-2}$. (b) The phase transition for a system at $\eta = 2$ when varying density as a control parameter. N was kept constant as L was varied to change the density. The data corresponds to \circ : $N = 40$, 101 ensemble averages; \square : $N = 100$, 100 ensemble averages; \triangle : $N = 400$, 12 ensemble averages. ρ is in units of L^{-2} .

whether there is an alternative control parameter to the density for the topological model. The density is a control parameter in the Vicsek model, when the alignment is based on how many agents there are within a given radius. It is logical to assume that

varying k could act as a control parameter in the topological model, when alignment depends the closest neighbours. The results of a potentially novel phase transition are portrayed in Fig. 11.

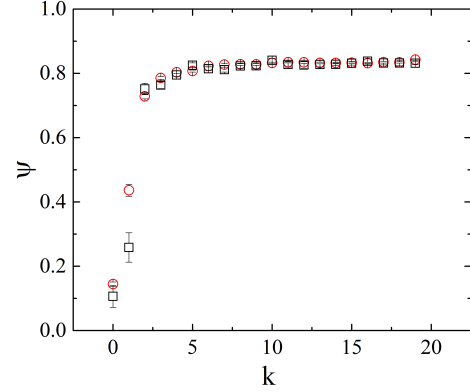


Figure 11: Effect of varying k (nearest neighbours) as a control parameter, on the order parameter ψ in the topological model. A phase transition is observed for $\eta = 2, N = 40, L = 3.1$ with 101 ensemble averages (\circ) and for $\eta = 2, N = 100, L = 5$ with 6 ensemble averages (\square).

The topological and Vicsek models have displayed similar results. A natural continuation would be to investigate whether there are any consistencies between the models.

The average number of nearest neighbours within R in the Vicsek model can be calculated. For $\rho = 4, k = 18$ was found to be 18 on average. The topological model with $k = 7$ and $k = 18$ are both compared to the Vicsek model as seen in Fig. 12. Evidently, when $k = 18$, the model is more similar to the Vicsek model, showing a consistency between the models. Since this has

not been investigated for larger systems, it is not necessarily true that the consistency would hold if the system size were increased. It is also important to note that $k = 18$ is just an average as this value is an integer and is not constant throughout the simulation.

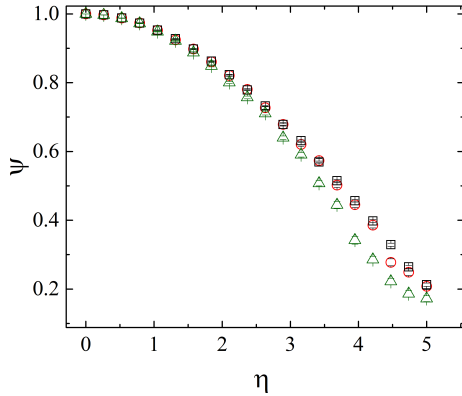


Figure 12: Comparison between the Vicsek model, the topological model with $k = 7$ and $k = 18$. The Vicsek model (\square) corresponds with the topological model when $k = 18$ (\circ) whilst when $k = 7$ the phase transition is steeper (\triangle). Averages were taken across: 18 nearest neighbours - 101 repeats, Vicsek model - 461 repeats, 7 nearest neighbours - 101 repeats. All for system $N = 40$, $L = 3.1$

B. Rotors

After immersing an asymmetric rotor in an active bath of no alignment interactions ($\alpha = 0$) and $\eta = 0$, it was confirmed that it rotates spontaneously due to the active agents in the bath. This was expected due to the symmetry breaking of time and space as mentioned in the theory. The rotor has positive angular velocity when antisymmetric to the right and negative when asym-

metric to the left as shown in Fig. 13. For a symmetric rotor, no rotation is observed because the shape of the rotor no longer breaks space symmetry.

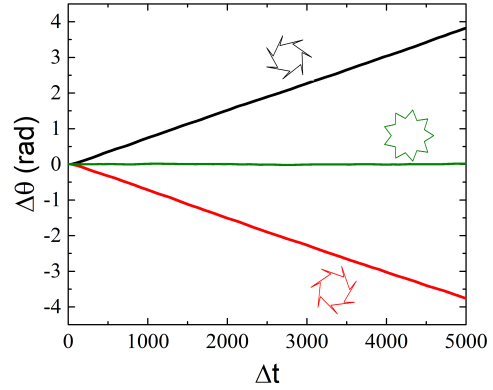


Figure 13: Angular displacement ($\Delta\theta$) for $U = 5000$ showing that asymmetric shapes rotate and symmetric do not. Red line is when the shape is antisymmetric to the left, black line is when the shape is antisymmetric to the right, green line is when the shape is symmetric. All lines are ensemble averaged 96 times.

Next, alignment interactions between the particles were turned on ($\alpha = 1$) and it was noticed that the rotor has a significantly higher angular displacement as seen by the red data in Fig. 14a, than when ($\alpha = 0$). An explanation could be that the system is further away from equilibrium, so the rectification effect is significantly enhanced due to collective motion.

Results for the angular displacement when $\alpha = 1$ and $\alpha = 0$ were all obtained. These were repeated for $\eta = 2$, Fig. 14b, and for $\eta = 5$, Fig. 14c. Evidently, as noise is increased, the end angular displacement of asymmetric rotors decreases.

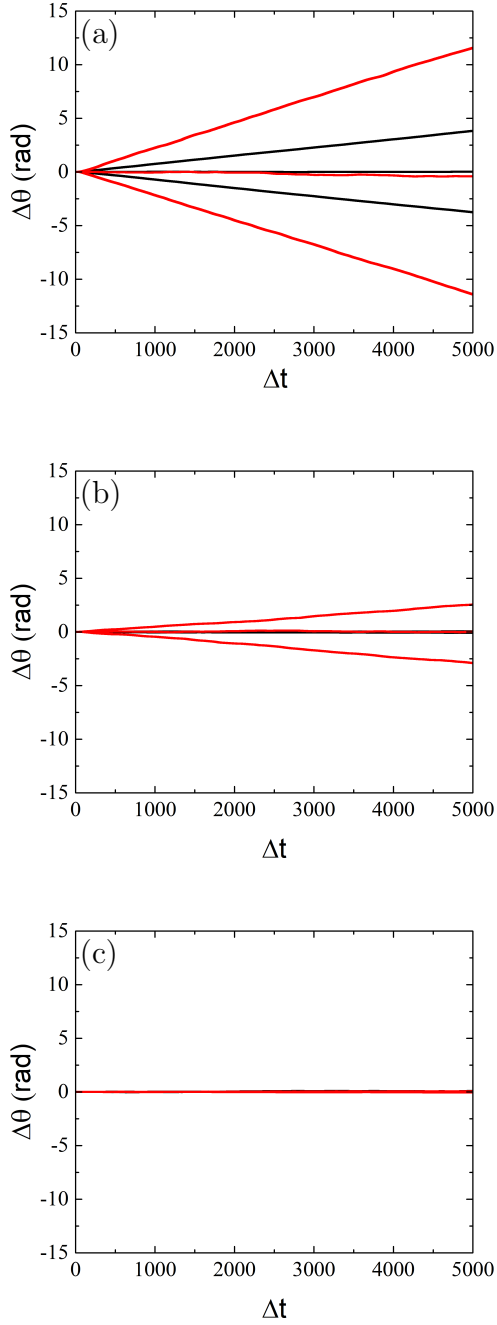


Figure 14: Angular displacement ($\Delta\theta$) for $U = 5000$ for three rotors: a symmetric, asymmetric to the left, asymmetric to the right. All rotations are recorded with $\alpha = 1$ (red) and $\alpha = 0$ (black). (a) $\eta = 0$. For symmetric shape $\Delta\theta \approx 0$. For asymmetric shapes $\Delta\theta \neq 0$. (b) $\eta = 2$. Only asymmetric shapes with $\alpha = 1$ have $\Delta\theta \neq 0$. (c) $\eta = 5$. $\Delta\theta = 0$ for all shapes. All results are 96 ensemble averages.

When noise is high ($\eta = 5$), the angular displacement of all shapes in all baths, is ap-

proximately zero. This suggests that time symmetry is no longer broken. An explanation could be that the noise is large enough to overwhelm the self-propulsion of the particles, causing them to act as passive particles which have thermal excitations.

Furthermore, there is an evident non-linear relationship between noise and rotation of the rotor which was explored in detail as shown in Fig. 15.

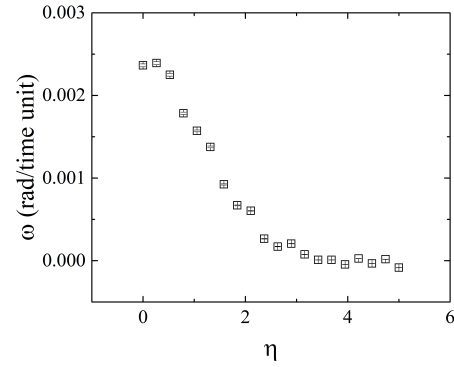


Figure 15: Phase transition of η as control parameter and ω as an order parameter. As η is increased, there is a decrease in the rotation of the shape. 420 ensemble averages were taken.

This resembles the phase transitions studied for the topological and Vicsek model but with ω as an order parameter. This led to a question to be asked: is there a relationship between ω and ψ ? So, is there an x that can satisfy

$$\omega \approx \psi^x \quad (8)$$

To answer this question, the phase transition in Fig. 15 was rescaled to be between 0 and 1. Then a least-squares approach was used by minimising the function

$$f(x) = \sum_{i=1}^n (\psi^x - w_i)^2 \quad (9)$$

This gave a value of $x = 6.7$, which can be inserted into Eq. 8. This scales the phase transition for ψ onto the phase transition for ω as seen in Fig. 16. From Eq. 9, the error of the resemblance is ≈ 0.025 .

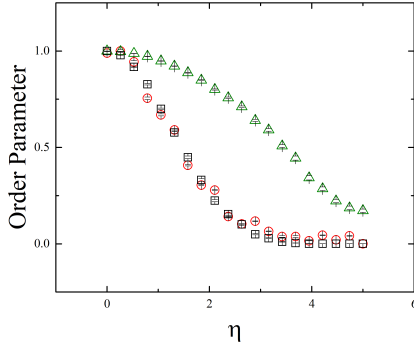


Figure 16: Mapping topological phase transition to novel rotation phase transition. The order parameter ψ in the topological phase transition (\triangle) for $k = 7$, is raised to the power 6.7 (\circ). The order parameter ω for the rotation phase transition is scaled between 0 (\square).

There is an empirical relationship between the order parameters ω and ψ , as η is varied as a control parameter. This suggests that there is a quantitative way of relating order within an active system and rotation of an asymmetric object within the active bath. Perhaps unexpectedly, rotation scales as a higher power, (≈ 6.7), of the order, rather than linearly, which could mean something deeper about how the active nature of the particles affects rotation.

C. Genetic Algorithm

Finally, the genetic algorithm was used to optimise the shape of a rotor in a bath with $\alpha = 1$ and with $\alpha = 0$, each with $\eta = 0$ and $\eta = 2$. A visual example of how one of our populations (for $\alpha = 1$ and $\eta = 0$) evolves is portrayed in Fig. 17, for increasing generations of 0, 4, 7, 10, 19.

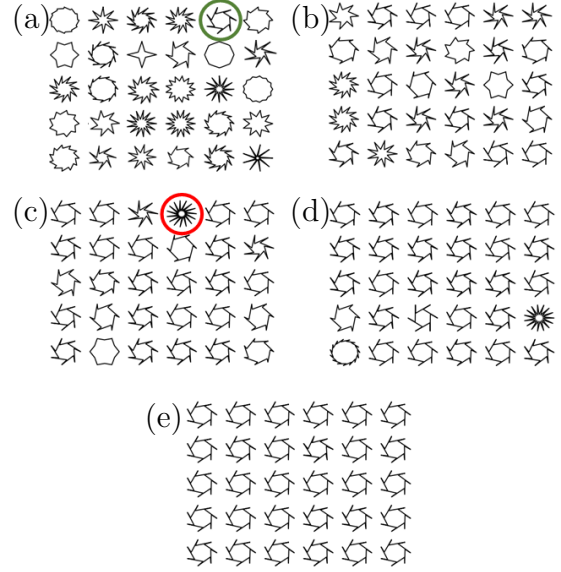


Figure 17: A population with parameters $\alpha = 1$ and $\eta = 0$ evolving for generation numbers of 0, 4, 7, 10, 19. (a) Population is initialised with optimal shape circled in green (b) Generation number 4. (c) Generation number 7 with a mutation circled in red that was not present in generation number 4. (d) Generation number 10 (e) Generation number 19 with optimal shape covering all of the population.

As the population is initialised, it contains 30 random members. As the generation number increases, the shapes created from parents with optimal scores become more prominent. An example of a mutation can be noticed at the 7th generation which was not present at the 4th genera-

tion. The optimal shape that is achieved in Fig. 17e is circled in green in the initial population in 17a. It can be observed how this shape becomes more prominent at each generation.

The results from the genetic algorithm can be seen in Fig. 18. Observing the results, it is evident that they confirm that collective motion, in particular alignment interactions, have a significant effect on rotation, as average displacement for the population is higher. It can also be seen that as the population is initialised, the scores are consistently low, but with each generation, they improve. This shows that the genetic algorithm is a suitable method for determining an optimal shape.

For each active bath, a best shape was achieved and the optimal shapes with their respective parameters are shown in Table 2.

Table 2 shows that the optimal shapes for $\alpha = 1$ are similar despite having different noise values. This could suggest that noise does not have a large impact on the optimal shape. This is further supported by the shapes for $\alpha = 0$, which are also similar with the only significant difference being S .

It can also be observed that all shapes have $a \approx \frac{2}{3}b$, suggesting that there is an optimal value for the inner radius, independent of the active bath. The angles are numerically different due to how the rotor is built, however visually they closely resem-

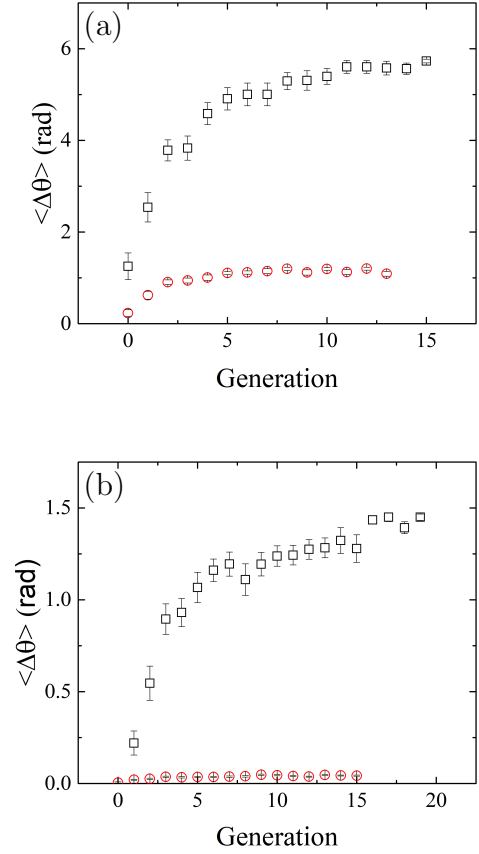


Figure 18: Genetic algorithms for different baths showing the average displacement of the population with each generation. (a) Genetic algorithm with $\alpha = 1$ and $\eta = 0$ (□), $\eta = 2$ (○) (b) Genetic algorithm with $\alpha = 0$ and $\eta = 0$ (□), $\eta = 2$ (○).

ble each other. For instance for $\alpha = 1$, the shapes appear to be nearly identical despite having very different ϵ .

V. Conclusions

The physics of collective motion has been explored in detail since Vicsek's seminal work in 1995. Apart from confirming his findings, this report showed evidence for a potential novel phase transition between a control parameter k and the order param-





Active Bath	Parameter Values	Optimal Shape
$\alpha = 0$ $\eta = 0$	$a = 0.641$ $\epsilon = 5.96$ $S = 11$	
$\alpha = 0$ $\eta = 2$	$a = 0.745$ $\epsilon = 1.49$ $S = 15$	
$\alpha = 1$ $\eta = 0$	$a = 0.761$ $\epsilon = 0.308$ $S = 7$	
$\alpha = 1$ $\eta = 2$	$a = 0.700$ $\epsilon = 5.77$ $S = 7$	

Table 2: Summary of optimal shapes and their parameters.

eter ψ . An interesting correspondence was shown between the Vicsek model and the topological model that could be explored further in an investigation of the resemblances between the two models.

The most exciting work done in this report was the immersion of the rotors in the active baths. With the aim of investigating what factors maximise the rotations (or potential to harness energy), we managed to find an optimal shape for different active baths using the genetic algorithm. The final shapes suggested that having an approximate ratio of 2:3, inner to outer radius is optimal for any active bath but the number of spikes depends on whether alignment interactions are on.

Furthermore, interesting results were obtained showing that alignment and noise significantly affect the rotation of the asymmetric shape. Specifically, an empirical relationship between ψ and ω was shown, which if allowed more time, could be developed into investigating the underlying reasons of this intriguing relationship. Therefore, the outlook looks extremely positive, as there is potential for a lot of research regarding the effect of collective motion on harnessing energy.

References

- [1] Sriram Ramaswamy. The mechanics and statistics of active matter. *Annu. Rev. Condens. Matter Phys.*, 1(1):323–345, 2010.
- [2] Julia K Parrish and William M Hamner. *Animal groups in three dimensions: how species aggregate*. Cambridge University Press, 1997.
- [3] Francesco Ginelli, Fernando Peruani, Marie-Hélène Pillot, Hugues Chaté, Guy Theraulaz, and Richard Bon. Intermittent collective dynamics emerge from conflicting imperatives in sheep herds. *Proceedings of the National Academy of Sciences*, 112(41):12729–12734, 2015.
- [4] He-Peng Zhang, Avraham Be’er, E-L Florin, and Harry L Swinney. Collective motion and density fluctuations in bacterial colonies. *Proceedings of the National Academy of Sciences*, 107(31):13626–13630, 2010.
- [5] Michael E Cates. Diffusive transport without detailed balance in motile bacteria: does microbiology need statistical physics? *Reports on Progress in Physics*, 75(4):042601, 2012.
- [6] Stephen J Ebbens and Jonathan R Howse. In pursuit of propulsion at the nanoscale. *Soft Matter*, 6(4):726–738, 2010.
- [7] Craig W Reynolds. Flocks, herds and schools: A distributed behavioral model. In *ACM SIGGRAPH computer graphics*, volume 21, pages 25–34. ACM, 1987.
- [8] Tamás Vicsek, András Czirók, Eshel Ben-Jacob, Inon Cohen, and Ofer Shochet. Novel type of phase transition in a system of self-driven particles. *Physical review letters*, 75(6):1226, 1995.
- [9] Walter F Paxton, Kevin C Kistler, Christine C Olmeda, Ayusman Sen, Sarah K St. Angelo, Yanyan Cao, Thomas E Mallouk, Paul E Lamert, and Vincent H Crespi. Catalytic nanomotors: autonomous movement of striped nanorods. *Journal of the American Chemical Society*, 126(41):13424–13431, 2004.
- [10] Rémi Dreyfus, Jean Baudry, Marcus L Roper, Marc Fermigier, Howard A Stone, and Jérôme Bibette. Microscopic artificial swimmers. *Nature*, 437(7060):862, 2005.
- [11] Loai KEA Abdelmohsen, Fei Peng, Yingfeng Tu, and Daniela A Wilson. Micro-and nano-motors for biomedical applications. *Journal of Materials Chemistry B*, 2(17):2395–2408, 2014.

- [12] Bradley J Nelson, Ioannis K Kaliakatos, and Jake J Abbott. Microrobots for minimally invasive medicine. *Annual review of biomedical engineering*, 12:55–85, 2010.
- [13] SJ Ebbens. Active colloids: Progress and challenges towards realising autonomous applications. *Current Opinion in Colloid & Interface Science*, 21:14–23, 2016.
- [14] R Di Leonardo, L Angelani, D Dell’Arciprete, Giancarlo Ruocco, V Iebba, S Schippa, MP Conte, F Mearini, F De Angelis, and E Di Fabrizio. Bacterial ratchet motors. *Proceedings of the National Academy of Sciences*, 107(21):9541–9545, 2010.
- [15] Andrey Sokolov, Mario M Apodaca, Bartosz A Grzybowski, and Igor S Aranson. Swimming bacteria power microscopic gears. *Proceedings of the National Academy of Sciences*, 107(3):969–974, 2010.
- [16] Peter Galajda, Juan Keymer, Paul Chaikin, and Robert Austin. A wall of funnels concentrates swimming bacteria. *Journal of bacteriology*, 189(23):8704–8707, 2007.
- [17] Dušan Babič, Carmen Schmitt, and Clemens Bechinger. Colloids as model systems for problems in statistical physics. *Chaos: An Interdisciplinary Journal of Nonlinear Science*, 15(2):026114, 2005.
- [18] Ivo Buttinoni, Giovanni Volpe, Felix Kümmel, Giorgio Volpe, and Clemens Bechinger. Active brownian motion tunable by light. *Journal of Physics: Condensed Matter*, 24(28):284129, 2012.
- [19] Hong-Ren Jiang, Natsuhiko Yoshinaga, and Masaki Sano. Active motion of a janus particle by self-thermophoresis in a defocused laser beam. *Physical review letters*, 105(26):268302, 2010.
- [20] Howard C Berg. *E. coli in Motion*. Springer Science & Business Media, 2008.
- [21] Howard C Berg and Linda Turner. Chemotaxis of bacteria in glass capillary arrays. *escherichia coli*, motility, microchannel plate, and light scattering. *Biophysical Journal*, 58(4):919–930, 1990.
- [22] N Koumakis, C Maggi, and R Di Leonardo. Directed transport of active particles over asymmetric energy barriers. *Soft matter*, 10(31):5695–5701, 2014.

- [23] Clemens Bechinger, Roberto Di Leonardo, Hartmut Löwen, Charles Reichhardt, Giorgio Volpe, and Giovanni Volpe. Active particles in complex and crowded environments. *Reviews of Modern Physics*, 88(4):045006, 2016.
- [24] Tamas Vicsek. A question of scale. *Nature*, 411(6836):421, 2001.
- [25] Reynolds boids computer program. <http://www.red3d.com/cwr/boids/>. Accessed: 2019-03-13.
- [26] Eric Bertin, Michel Droz, and Guillaume Grégoire. Hydrodynamic equations for self-propelled particles: microscopic derivation and stability analysis. *Journal of Physics A: Mathematical and Theoretical*, 42(44):445001, 2009.
- [27] Roland Bouffanais. *Design and control of swarm dynamics*. Springer, 2016.
- [28] Guillaume Grégoire and Hugues Chaté. Onset of collective and cohesive motion. *Physical review letters*, 92(2):025702, 2004.
- [29] Máté Nagy, István Daruka, and Tamás Vicsek. New aspects of the continuous phase transition in the scalar noise model (snm) of collective motion. *Physica A: Statistical Mechan-*
- ics and its Applications*, 373:445–454, 2007.
- [30] Hugues Chaté, Francesco Ginelli, Guillaume Grégoire, and Franck Raynaud. Collective motion of self-propelled particles interacting without cohesion. *Physical Review E*, 77(4):046113, 2008.
- [31] Francesco Ginelli. The physics of the vicsek model. *The European Physical Journal Special Topics*, 225(11-12):2099–2117, 2016.
- [32] Michele Ballerini, Nicola Cabibbo, Raphael Candelier, Andrea Cavagna, Evaristo Cisbani, Irene Giardina, Vivien Lecomte, Alberto Orlandi, Giorgio Parisi, Andrea Procaccini, et al. Interaction ruling animal collective behavior depends on topological rather than metric distance: Evidence from a field study. *Proceedings of the national academy of sciences*, 105(4):1232–1237, 2008.
- [33] Francesco Ginelli and Hugues Chaté. Relevance of metric-free interactions in flocking phenomena. *Physical Review Letters*, 105(16):168103, 2010.
- [34] Guillaume Grégoire, Hugues Chaté, and Yuhai Tu. Moving and staying together without a leader. *Physica D: Nonlinear Phenomena*, 181(3-4):157–170, 2003.

- [35] Yaouen Fily and M Cristina Marchetti. Athermal phase separation of self-propelled particles with no alignment. *Physical review letters*, 108(23):235702, 2012.
- [36] Xiao-Lun Wu and Albert Libchaber. Particle diffusion in a quasi-two-dimensional bacterial bath. *Physical review letters*, 84(13):3017, 2000.
- [37] L Angelani, C Maggi, ML Bernardini, A Rizzo, and R Di Leonardo. Effective interactions between colloidal particles suspended in a bath of swimming cells. *Physical review letters*, 107(13):138302, 2011.
- [38] Andreas Kaiser, Anton Peshkov, Andrey Sokolov, Borge Ten Hagen, Hartmut Löwen, and Igor S Aranson. Transport powered by bacterial turbulence. *Physical review letters*, 112(15):158101, 2014.
- [39] SA Mallory, C Valeriani, and A Cacciuto. Curvature-induced activation of a passive tracer in an active bath. *Physical Review E*, 90(3):032309, 2014.
- [40] Frank Smallenburg and Hartmut Löwen. Swim pressure on walls with curves and corners. *Physical Review E*, 92(3):032304, 2015.
- [41] Richard P Feynman, Robert B Leighton, and Matthew Sands. The feynman lectures on physics: Ratchet and pawl vol. 1, chap. 46, 1966.
- [42] Luca Angelani, Roberto Di Leonardo, and Giancarlo Ruocco. Self-starting micromotors in a bacterial bath. *Physical review letters*, 102(4):048104, 2009.
- [43] He Li and HP Zhang. Asymmetric gear rectifies random robot motion. *EPL (Europhysics Letters)*, 102(5):50007, 2013.
- [44] Claudio Maggi, Julianne Simmchen, Filippo Saglimbeni, Jaideep Katuri, Michele Dipalo, Francesco De Angelis, Samuel Sanchez, and Roberto Di Leonardo. Self-assembly of micro-machining systems powered by janus micromotors. *Small*, 12(4):446–451, 2016.
- [45] Github project. <https://github.com/LNS98/swarming-project>. Accessed: 2019-03-13.